Light emission from direct and phonon-assisted processes in AlGaAs/GaAs HBT's

S. Villa, A. L. Lacaita, A. Di Carlo* and P.Lugli*
Politecnico di Milano, Dipartimento di Elettronica e Informazione and CEQSE-CNR,
Piazza L. da Vinci 32, 20133 Milano (Italy)
*Universitá di Roma "Tor Vergata", Dipartimento di Ingegneria Elettronica,
Via della Ricerca Scientifica, 00133 Roma (Italy)

April 29, 1996

Abstract

In this work we present a calculation of electroluminescence spectra from an AlGaAs/GaAs heterojunction bipolar transistor (HBT) over the near-infrared and visible range (0.8-2.5 eV) obtained coupling a self-consistent Monte Carlo with minority carrier transport simulation to a nonlocal-pseudopotential algorithm. We compute both direct and phonon-assisted optical transition rates.

Introduction

A great deal of theoretical and experimental effort has been devoted to the interpretation of hot-electron induced effects in electron devices under high electric fields. In such situations carrier distribution strongly departs from maxwellian equilibrium shape, carrier kinetic energy can reach values as high as 2–3 eV, impact ionization phenomena and band structure effects begin to play a fundamental role in their dynamics. In order to analyze carrier transport, full-band Monte Carlo (MC) simulators have been developed.

Consistency checks of their transport models have been performed by comparing measurements with predictions of steady state and electrical transients.

However the bare caracterization of the currents at the contacts gives poor information on hot carrier population because currents are physical quantities depending on the behaviour of the whole electron population, therefore other effects more directly related to the hot carrier population have been searched for.

More recently, the optical characterization of semiconductor devices by means of electroluminescence (EL) spectra measurements have become fairly accurate and reproducible; provided that the transition rates for all carrier radiative relaxation processes were properly computed, energy-resolved information on carrier distribution can be retrieved from the spectral analysis of emitted light.

The most interesting applications of these effects have been found in device diagnostics and reliability area: EL spectra from semiconductor devices have been correlated with their electrical characteristics and their stress conditions. On the other hand, common device faults such as breakdown microplasmas are often connected to anomalies in the emission spectra. The same phenomena can be useful to test MC predictions as long as a quantitative model of light emission mechanisms makes possible to link detected spectra to carrier distribution function. In spite of the renewed efforts recently devoted to the topic, the model of hot carrier radiative relaxation still remains an open question.

More in detail, there are three kind of scattering processes responsible for photon emission: direct (k-conserving) transitions, phonon-assisted transitions and ionized-impurity assisted processes (usually referred as Bremsstrahlung radiation). Since the work of Figielsky and Torun [1] bremsstrahlung was regarded as the one playing the main role, but in the last years it has been shown both theoretically and experimentally [2, 3, 4, 5] that it gives negligible effect in non-degenerate semiconductors, so in many works only direct processes have been considered in the computations. However it has been recently shown that phonon-assisted transitions play a significant role in the emission from silicon devices [6, 5].

In this work we present a complete theoretical analysis of light emission in GaAs including intraband and interband radiative processes.

Theoretical framework

A. Radiative processes modelling

Fig. 1 schematically shows the three transition processes we will deal with in this work: the first-order transition from $|1\rangle$ to $|2\rangle$ is a direct k−conserving transition, the two-step transition $|1'\rangle \rightarrow |1\rangle \rightarrow |2\rangle$ is a phonon-assisted process that classically corresponds to the sequence of two scattering events in which the electron-phonon scattering precedes the electron-photon scattering, in the following we will label it a "phonon-photon process"; finally the transition $|1\rangle \rightarrow |2\rangle \rightarrow |2'\rangle$ is the second-order process that we will label "photon-phonon"; in this case the time sequence of the electron-phonon and electron-photon scattering events has been reversed. It seems clear that the three processes shown in Fig. 1, altough represented by different mathematical terms, basically share the same physical process: the direct transition $|1\rangle \rightarrow |2\rangle$.

B. Direct processes

In the commonly used first-order approximation the emission rate per carrier per unit energy, time and crystal volume obtained integrating all direct transition probabilities is [8]

$$W(\hbar\omega) = \frac{8ne^2\hbar\omega}{3m^2c^3\Omega}C(\omega)\sum_{\nu,\nu',\mathbf{k}}|\hbar\langle\nu',\mathbf{k}|\nabla|\nu,\mathbf{k}\rangle|^2 \times$$
$$f(E_{\nu',\mathbf{k}})(1-f(E_{\nu,\mathbf{k}}))\delta(E_{\nu',\mathbf{k}}-E_{\nu,\mathbf{k}}-\hbar\omega) \qquad (1)$$

where we have denoted with Ω the volume, $|\nu,\mathbf{k}\rangle$ is the Bloch eigenstate of crystal momentum $\mathbf{k}$ and band index ν, $f(E)$ is the energy-dependent electron probability distribution and $C(\omega)$ is a corrective factor given by

$$\left|1+\frac{\omega}{n}\frac{dn}{d\omega}\right| \qquad (2)$$

that accounts for corrections in the optical density of states when frequency-dependences of the refractive index n are considered [6].

C. Phonon assisted processes

Since quantum interference phenomena can be neglected we compute phonon-assisted radiative scattering rates summing the transition probabilities for all possible phonon-assisted process; for the example drawn in Fig. 1 the squared matrix element for the transition $|1'\rangle \rightarrow |1\rangle \rightarrow |2\rangle$ is

$$\left|\frac{\langle 2|H_\omega|1\rangle\langle 1|H_0|1'\rangle}{E_1+\hbar\omega_0-E_{1'}+i\Gamma_{1'}}\right|^2, \qquad (3)$$

while the matrix element for the transition $|1\rangle \rightarrow |2\rangle \rightarrow |2'\rangle$ is given by

$$\left|\frac{\langle 2'|H_0|2\rangle\langle 2|H_\omega|1\rangle}{E_2+\hbar\omega-E_1+i\Gamma_1}\right|^2 \qquad (4)$$

where H_0 is the electron-phonon hamiltonian, H_ω is the electron-photon one, $\hbar\omega$ and $\hbar\omega_0$ are the energies of the photon and the phonon respectively.

It is worth noting that our matrix elements differ from these of Ref [5] because we have accounted for the effect of finite initial state lifetime in the transition probabilities introducing the state energy width Γ in the denominators: this refinement has allowed us to achieve a greater numerical stability in the algorithm. A more complete description of the second-order integration algorithm we use is given in full detail in Ref [6].

D. Total emission

According to the standard perturbation theory we could obtain the total emission simply summing up the direct and indirect emission as calculated from the previously described models. However, following this approach we would overcount the contribution due to direct transitions. As an example, the direct transition in Fig. 1 is counted three times: the first time as a direct transition; the second in the sum of all "sequential phonon-photon" transitions where the intermediate state is $|1\rangle$ and the final is $|2\rangle$ and the third time in the sum of all "sequential photon-phonon" processes sharing the initial state $|1\rangle$ and the intermediate state $|2\rangle$. This inconvenience is due

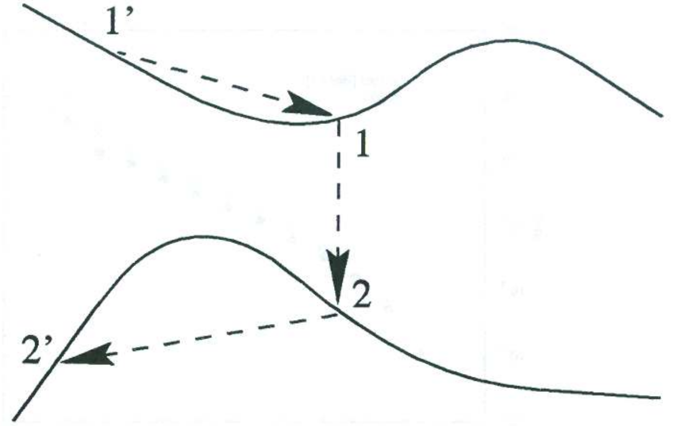

Figure 1: Schematic of first and second-order radiative processes

to the fact that in our case second-order terms implicitely include first order terms, but on the other hand the physics is refined.

For example, it will be even more refined to calculate emission rates from the third-order theory summing the probabilities of emission processes arising from "phonon-photon-phonon" transitions such as $|1'\rangle \rightarrow |1\rangle \rightarrow |2\rangle \rightarrow |2'\rangle$. In this way we would include all phonon-assisted processes and at the same time we would naturally account for initial-state and final-state decay of the direct transition $|1\rangle \rightarrow |2\rangle$.

However, we can have a good estimate even retaining the second-order framework; since the kinetic energy of the initial state $|1\rangle$ is usually higher than that of the final state $|2\rangle$, the corresponding broadening is also higher, it can then be assumed that most part of the broadening effects arise from initial-state lifetime, while final-state lifetime could be neglected. Under this assumption the essential physics of the process is described in the "phonon-photon" term that, besides including assisted processes, naturally describes the build-up of the state $|1\rangle$.

Finally, note that in this framework the distinction between pure direct transitions and phonon-assisted ones is somewhat arbitrary and difficult to define because only a complete non-perturbative treatment of quasiparticle properties of electron states could allow us to distinguish properly the sequence of two allowed transitions from one single second-order process.

Numerical implementation

The Monte Carlo program used to simulate carrier transport into the device is fully described in Ref [7]; it consists in a self-consistent one-dimensional Poisson-Monte Carlo solver in which the GaAs band structure has been fitted by a non-parabolic analytical model consisting in a three-valleys conduction band and three valence bands. All relevant phonon, ionized impurity and carrier-carrier scattering mechanisms have been included and impact ionization has been modelled by an extension of Kane's model to GaAs; a properly suited

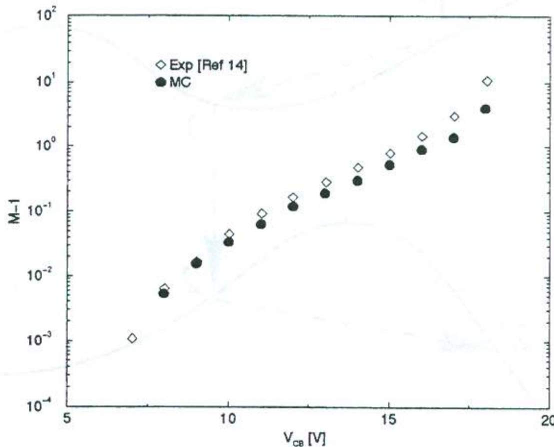

Figure 2: Comparison of the calculated M-1 multiplication factors with the measures from Ref[14]

weighted algorithm is used to improve efficiency when simulating devices in avalanche breakdown regime.

The emission has been computed by using "phonon-photon" term including in the numerical algorithm only the first term of Eq.(21) in Ref [6]. The Bloch eigenstates and momentum matrix elements have been obtained from a non-local empirical pseudopotential program that accounts for spin-orbit splittings using a potential in the form introduced by Chelikowsky *et al.* [9]. The wavevector sums over the Brillouin zone were carried out with an hystogram integration method using a uniform mesh that includes 60951 points in the irreducible wedge. The summations over band indexes have to be done over all the band of interest here; we have used 8 valence and 8 conduction bands computing both transitions within different conduction (*cc*-transitions) or valence (*vv*-transitions) bands and radiative recombinations (*cv*-transitions).

The device

The simulated device is an MBE-grown *n-p-n* AlGaAs/GaAs HBT with graded emitter, it is composed of a 80 nm n-layer ($5 \times 10^{18}\text{cm}^{-3}$) collector contact followed by a 500 nm n-GaAs ($2.5 \times 10^{16}\text{cm}^{-3}$) collector and a 120 nm p-GaAs base ($2 \times 10^{19}\text{cm}^{-3}$); the AlGaAs($5 \times 10^{17}\text{cm}^{-3}$) emitter region is compositionally graded near the base in order to reduce the conduction band step at the base-emitter junction. The epilayer is etched to form a two-level mesa structure with an emitter diameter of 100 μm. In order to perform optical measurements on the device a circular hole of about 30μm diameter was opened in the emitter metallization.

The results

We have simulated the emission from the device biased in forward active region with V_{cb} biases ranging from 10V (where there is a significant onset of hot-carrier induced light emission) to 18V (where a pre-breakdown regime at the collector-base junction is reached). Under these conditions electron-hole pairs are generated by impact ionization in the CB space-charge region, the holes are then injected into the base layer giving a negative contribution to the base current; a first check upon the carrier distributions obtained from the MC program can be obtained extracting the multiplication factor $(M - 1)$ from a measure of the base current[10]; as shown in Fig. 2 the agreement is good.

A. Cold carrier emission

Radiative recombination between cold carriers located in the base region contribute to the light emission from the device giving a sharply peaked recombination spectrum with a thermal tail that dominates in the energy range from the bandgap to about 1.9 eV. The form and intensity of this peak does not present appreciable variations with respect to the collector bias; as shown in Ref [11] this peak remains practically the same for any reverse V_{cb} while keeping constant the emitter current. Light emission from cold carriers can then be obtained in a separate manner simply by measuring device emission at $V_{cb} = 0$. We have included in the simulation cold-carrier emissions also, our results showed that first and second-order approach give similar results; the only differences were given by the fact that indirect emission rises more sharply at the bandgap and its tail has a slightly greater magnitude but still remains quasi-thermal. This result suggests that radiative recombinations in the base of the device can easily be explained by first-order approximation and there is no need to account for second-order corrections. In addition results obtained from second-order algorithm show some numerical oscillation due to problems with too cold carrier distributions; the results that we will show in the following have been obtained including $c - v$ radiation spectra obtained from first-order algorithm only.

It is worth noting that we haven't found the secondary peak located at 2.09 eV observed by Zanoni et al; altough similar peaks has been seen also in photoluminescence from heavily doped GaAs layers[12, 13] and have been attributed to an $L_{6c} - \Gamma_{7v}$ transition, such an explanation could be questionable. In order to get a quantitative description of the details of cold carrier emission near the gap region, an *ad hoc* algorithm should be designed for the purpose and low energy phenomena such as the existence of excitons should be accounted for; in device applications oriented toward hot carrier analysis however these details are absolutely negligible.

B. Hot carrier emission

In Fig. 3 we show the emission spectra for intraband transitions obtained from both first and second-order calculations for the device biased at V_{CB}=14V. As the figure clearly shows, the correction introduced by second-order approach

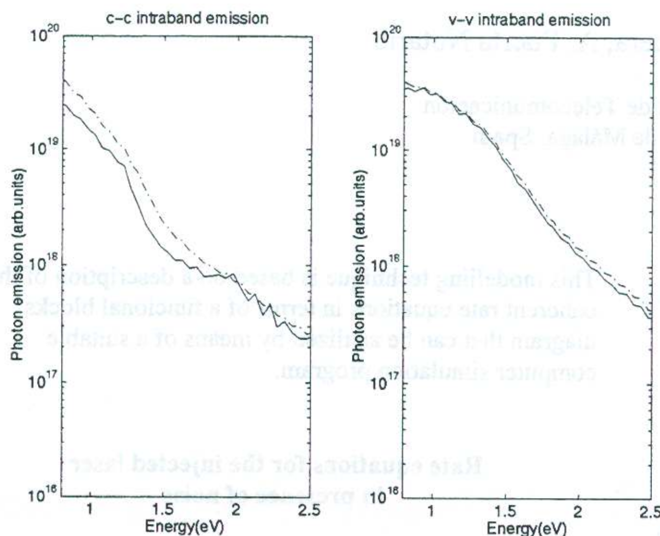

Figure 3: Comparison of first-order (continuous lines) and second-order (dashed-dotted lines) results at V_{CB}=14V

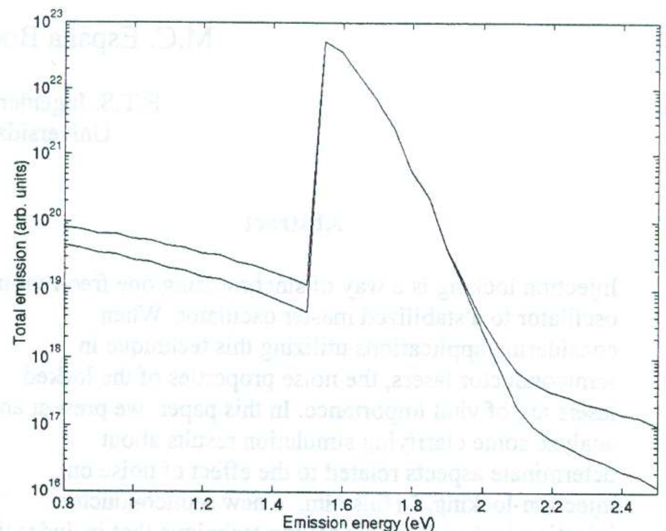

Figure 4: Total emission from the HBT at V_{CB}=10V and V_{CB}=14V

is far from being negligible in the computation of intra-conduction band transitions. On the other hand, while computing intra-valence band transitions this correction gives only quantitative refinements; it is worth noting that we have found the same behaviour at the other bias conditions we simulated too.

Altough a more extensive analysis on some different devices should be more appropriate, our results suggest that second-order corrections play a fundamental role in hot electron emission while direct transitions framework could give reasonable results when only hot hole emission is considerable. More in detail we can also see that, in contrast to what found in silicon devices, second-order corrections are most important in the low-energy part of the spectrum.

Fig. 4 shows the total emission from the device that we obtain from the calculations when corrections for light reabsorption in the top layers of the device are accounted for; the comparison with the experimental data from Ref[14] is good.

Conclusions

We have presented a complete theoretical model of photon emission from gallium arsenide devices including all relevant radiative processes. Our results show that the use of a second order formalism in the simulation of light emission from GaAs devices introduces considerable corrections with respect to the results obtained from a first-order calculation of direct radiative transitions when most of the light comes from hot electrons, the effect is less noticeable when the emission is caused by hot hole relaxation.

When corrections for the reabsorption of light in the device are included a good agreement with the available experimental data is found. In order to improve the quantitative accuracy of the model some concerns about the use of the Fermi golden rule should be raised; the use of perturbation theory should be abandoned and a more complete framework based on a non-perturbative approach should be used.

Acknowledgements

This work was supported by the Italian Ministry of Scientific Research and Technology and the National Research Council.

References

1. T. Figielsky and A. Torun, in *Proc. Int. Conf. on the Physics of Semiconductors*, edited by A. Strickland (Institute of Physics, London, 1962), p. 863.
2. H. S. Wong, in *IEDM Technical Digest* (1991), p. 549.
3. H. S. Wong, Electron Device Letters **13**, 389 (1992).
4. A. Lacaita, F. Zappa, S. Bigliardi, and M. Manfredi, IEEE Transactions on Electron Devices **ED-40**, 577 (1993).
5. J. Bude, N. Sano, and A. Yoshii, Phys. Rev. B **45**, 5848 (1992).
6. S. Villa, A. L. Lacaita, and A. Pacelli, Phys. Rev. B **52**, 10993 (1995).
7. P.Lugli, Microelectron. Eng. **19**, 275 (1992).
8. H. Bebb and E. Williams, in *Semiconductor and Semimetals, Volume 8*, edited by R. K. Willardson and A. C. Beer (Academic Press, New York, 1992).
9. J. R. Chelikowsky and M. L. Cohen, Phys. Rev. B **14**, 556 (1976).
10. A. D. Carlo and P. Lugli, IEEE Electron Device Letters **14**, 103 (1992).
11. E. Zanoni *et al.*, Applied Physics Letters **62**, 402 (1993).
12. J. Sapriel *et al.*, Solid State Communications **79**, 543 (1991).
13. D. Olego and M. Cardona, Phys. Rev. B **22**, 886 (1980).
14. E. Zanoni *et al.*, IEEE Electron Device Letters **13**, 253-255 (1992).